ANTIOXIDANTS & REDOX SIGNALING
Volume 11, Number 8, 2009

DOI: 10.1089/ars.2009.2427

Original Research Communication

Superoxide Anion Regulates the Mitochondrial Free Ca^{2+} Through Uncoupling Proteins

Zhaofei Wu,[1,2] Jie Zhang,[3] and Baolu Zhao[1,2,4,5]

Abstract

Mitochondrial dysfunction, which is closely related to intracellular calcium overload and excessive free radicals, is an important cause of Alzheimer's disease (AD). However, molecular mechanisms of the mitochondrial Ca^{2+} disregulation induced by oxidative stress in AD are still obscure. In an effort to gain a further understanding of this problem, we investigated the effects of superoxide anion, a primary free radical, on the expression of uncoupling proteins (UCPs) and the mitochondrial free Ca^{2+} levels in the neuroblastoma SH-SY5Y cell line (neo) and stably expressed wild-type human APP(APP) and APP-Swedish mutation (APPsw) SH-SY5Y cells. It was found that UCP2 and UCP4 protein levels were upregulated in neo but downregulated in APP and APPsw cells by the superoxide anion. Our results show that the superoxide anion can regulate protein levels of UCP2 and UCP4 in SH-SY5Y cells, and the mitochondrial free Ca^{2+} shifted their levels, tightly coupled with the protein levels of UCPs. When UCP2 and UCP4 were knocked down by siRNA, the result was reversed. These data suggest that the superoxide anion can regulate the mitochondrial free Ca^{2+} by regulating the expression of UCPs. These observations also indicate that UCPs can be potential targets in pathotherapy prevention of AD. *Antioxid. Redox Signal.* 11, 1805–1818.

Introduction

Uncoupling proteins (UCPs) belong to the superfamily of mitochondrial ion-carrier proteins and are embedded in the inner mitochondrial membrane (29). UCP1, which is preferentially expressed in brown adipose tissue, accounts for heat production by inducing an H^+ leak that uncouples oxidative phosphorylation (29, 44). However, except for UCP1, the precise physiologic functions of UCPs have not yet been established. Interestingly, quite far from their original names, UCP2, UCP3 (52), and UCP4 (12), which have been identified in many tissues, were recently found to be involved in mitochondrial Ca^{2+} homeostasis. Strong evidence indicates that UCPs (UCP2, UCP4, and BMCP1/UCP5) have a profound influence on neuronal function. By regulating mitochondrial biogenesis, calcium flux, free radical production, and local temperature, neuronal UCPs can directly regulate neurotransmission, synaptic plasticity, and neurodegenerative processes (2, 25). Although the physiological role of UCPs is uncertain, their activation by superoxide free radicals suggests that UCPs are central to the mitochondrial response to reactive oxygen species (ROS) (21, 30, 38).

Not only are mitochondria the main organelle in which superoxide free radicals are generated, but mitochondria are also important Ca^{2+} pools (10, 24). Mitochondrial Ca^{2+} uptake is a crucial regulator of the oxidative phosphorylation rate, the modulation of spatiotemporal cytosolic Ca^{2+} signals, and apoptosis (24). Although the phenomenon of mitochondrial Ca^{2+} sequestration, its characteristics, and physiological consequences have been convincingly reported (11, 19, 27), the actual proteins involved in this process are still ambiguous.

Both increased oxidative stress and disordered mitochondrial Ca^{2+} in neurons have been tightly correlated with the incidence of Alzheimer's disease (AD) (9, 13, 14, 33, 37, 48, 49). It is reasonable to speculate that UCPs might play an intermediate role in the pathology of AD, through superoxide free

[1]State Key Laboratory of Brain and Cognitive Sciences, Institute of Biophysics, Chinese Academy of Sciences, and [2]Graduate University of the Chinese Academy of Sciences, Beijing, the P.R. China.
[3]Department of Cell Biology and Neuroscience, Rutgers University, Piscataway, New Jersey.
[4]Key Laboratory of Mental Health, Chinese Academy of Sciences, Beijing, and [5]Division of Nitric Oxide and Inflammatory Medicine, E-Institutes of Shanghai Universities, Shanghai University of Traditional Chinese Medicine, Shanghai, the P.R. China.

radicals and mitochondrial Ca^{2+}. The present work was designed to try to answer the following questions: How do superoxide free radicals affect the expression of UCPs? Do the levels of UCPs directly relate to mitochondrial Ca^{2+} homeostasis? Is the physiologic role of UCPs as mitochondrial Ca^{2+} transporters? Also, it should be determined whether the β-amyloid precursor protein (APP) takes a part in this alteration of neuronal mitochondrial Ca^{2+} homeostasis.

Materials and Methods

Cell culture and treatment

Stably transfected human neuroblastoma SH-SY5Y cell strains expressing wild-type human APP (APP), APP-Swedish mutation (APPsw), or vector (neo) only were established in our laboratory (58). These cell strains were cultured in Dulbecco's modified Eagle's medium (DMEM) supplemented with 10% heat-inactivated fetal calf serum, 100 IU/ml penicillin, and 100 μg/ml streptomycin at 37°C in a humidified, 5% CO_2 incubator. G418 (200 μg/ml) was added into the medium to maintain the genotypically stable cell strains.

Before the collection and detection of mitochondrial free Ca^{2+} and UCPs levels, the cells were stimulated with superoxide anion, incubated with either 50 m*M* xanthine plus xanthine oxidase (0.01 U per 3.5 ml) for 3 h or with 50 m*M* xanthine plus heat-inactive xanthine oxidase (0.01 U per 3.5 ml, heated at 100°C) for 3 h as a control (21). The production of superoxide anion in mitochondria with this method was detected with a newly developed superoxide anion–specific indicator protein, mito-cpYFP (57). To exclude any possible interference of H_2O_2, 20 U/ml of catalase (Sigma-Aldrich, USA) and 2.5 μ*M* deferoxamine mesylate (Novartis Pharma, Switzerland), which is an iron (III) chelator, were added into the medium (23).

Western blotting

The cells were lysed on ice in lysis buffer (20 m*M* Tris-HCl, pH 7.4, 2.5 m*M* EDTA, 1% Triton X-100, 1% sodium deoxycholate, 0.1% SDS, 100 m*M* NaCl, 10 m*M* NaF, 1 m*M* Na_3VO_4, 1 m*M* Pefabloc SC, 10 mg/ml aprotinin, 10 mg/ml leupeptin, and 10 mg/ml pepstatin A). Protein concentrations were determined by using a Bicinchoninic Acid (BCA) kit (Pierce, Rockford, IL). Total cell lysates were subjected to electrophoresis at an equal protein content per well on a 12% sodium dodecyl sulfate–polyacrylamide gel electrophoresis (SDS–PAGE) gel, followed by wet transfer of separated proteins to a BioTrace NT Pure Nitrocellulose Blotting Membrane (Pall Corporation, East Hills, NY). Membranes were blocked for 1.5 h in 4% skim milk in Tris-buffered saline with 0.1% Tween 20 (TBS-T) and subsequently incubated overnight at 4°C with primary antibodies (sc-6525 for hUCP2, sc-17582 for hUCP4, sc-1984 for PPAR-γ, and sc-47778 for β-actin; Santa Cruz, Santa Cruz, CA). The membranes were washed 3 times for 15 min each with TBS-T and incubated with horseradish peroxidase (HRP) conjugate secondary antibodies (sc-2768 and sc-2005; Santa Cruz) for 1 h at room temperature. The membranes were then washed 3 times with TBS-T for 15 min each and once with TBS for 5 min. The immunoreactive bands were visualized with enhanced chemiluminescence (ECL; Pierce, Rockford, IL). The intensity of immunoreactive bands was quantified by using an NIH Image tool.

Plasmids and DNA transfections

The ratiometric-pericam-mt in pcDNA 3 was a gift from Dr. Atsushi Miyawaki (Riken, Japan) (39). By following the manufacturer's guidelines, cells of ~60% confluency were transiently transfected with 0.3 μg of purified plasmid DNA by using SoFast (Sunma Biotechnology, Shenzhen, China). The mito-cpYFP in the pShuttle-CMV plasmid was generous provided by Prof. Heping Cheng (Peking University, China). Its transfection was carried out with Lipofectamine 2000 (Invitrogen, USA) by following the manufacturer's guidelines.

Measurement of mitochondrial membrane potential

Mitotracker Red is a noncytotoxic mitochondrion-specific dye that accumulates in mitochondria in a membrane potential–dependent manner. Mitochondrial membrane potential was determined in cultured cells by using the cell-permeable probe MitoTracker Red CMXRos (Molecular Probes, USA), as previously described (1).

Laser scanning confocal imaging of mitochondrial free Ca^{2+} concentrations in single cells

To monitor the mitochondrial free Ca^{2+} concentration ($[Ca^{2+}]_{mito}$), the cells were transfected with the mitochondria-targeted ratiometric-pericam (pericam-mt) and measured by using a FLUOVIEW FV500 confocal laser scanning biologic microscope (Olympus, Japan) for single-cell measurement. The pericam-mt was excited at 405 nm, and emission was collected at 535 nm. Thus, $[Ca^{2+}]_{mito}$ was expressed by the relative fluorescence intensity of the pericam-mt (34, 39).

Measurement of mitochondrial free Ca^{2+} concentrations by using a fluorescence microscope

To confirm the confocal results in a larger number of cells and to exclude any possible artifacts caused by the interaction between superoxide anion and the pericam-mt, the cells were loaded with rhod-2 acetoxymethyl ester (rhod-2 AM) in DMEM without fetal calf serum, at a concentration of 5 μ*M* for 30 min at room temperature. This was followed by three phosphate-buffered solution washes, and a 30-min incubation in DMEM at 37°C. Then the cells were illuminated at 540 nm, and fluorescence emission was collected at 605 nm (47, 51). Fluorescence was monitored on an OLYMPUS IX-71 fluorescence microscope equipped with an iXon-DV-897 EMCCD camera.

siRNA transfection

siRNAs were designed by online tools, the siDRM of the University of Minnesota and the BLOCK-iT RNAi Designer of Invitrogen, and chemicals were synthesized by GenePharma. The sequences against UCP2 were 5′-GGCCUGUAUGAUU CUGUCA-3′ (sense) and 5′-UGACAGAAUCAUACAGGCC-3′ (antisense), which were previously proved to be effective (52). The first pair of sequences against UCP4 was 5′-GCGAUUUCGUGGUGUACAU-3′ (sense) and 5′-AUGUA-CACCACGAAAUCGC-3′ (antisense). This 19-nucleotide sequence corresponds to position 504–522 of UCP4 (GenBank accession no. AF110532). The second pair of sequences against UCP4 was 5′-GGUAUUGAAUACACCACUU-3′ (sense) and 5′-AAGUGGUGUAUUCAAUACC-3′ (antisense). This 19-

nucleotide sequence corresponds to position 654–672 of UCP4. The sequences against APP were 5′-GCUGAUAAGA AGGCAGUUA-3′ (sense) and 5′-UAACUGCCUUCUUAU CAGC-3′ (antisense), which were also previously proved to be effective (22). An siRNA that does not target rat, mouse, or human genes was used as a negative control; the sequences are 5′-UUCUCCGAACGUGUCACGUTT-3′ and 5′-ACGUG ACACGUUCGGAGAATT-3′, respectively; these were provided by the manufacturer.

In brief, 1×10^5 cells/35-mm dish were plated and cultured under normal conditions described earlier until the cells reached ~80% confluency. The siRNAs were then transfected by using SoFast (Sunma Biotechnology) and by following the manufacturer's instructions. After 24 h, the cells were split into one six-well plate for treatment. Whole-cell extracts were obtained and subjected to Western blotting, as described earlier, to examine the expression of UCP2 and UCP4 protein. Additionally, some cells were trypsinized and assessed for $[Ca^{2+}]_{mito}$ by using a fluorospectrophotometer.

Statistics

Error bars represent the standard error of the mean (SEM). Asterisks indicate a significant difference from control, as determined with one-way ANOVA ($p < 0.05$).

Results

Differences in UCPs regulation among the cell strains by superoxide anion

We found that UCP2 and UCP4 protein levels were upregulated in SH-SY5Y (neo), which expresses only wild-type human APP, but downregulated by superoxide anion in SH-SY5Y (APP) and SH-SY5Y (APPsw) cell strains, which express excessive APP or APPsw, respectively. As previous shown, SH-SY5Y (APP) and SH-SY5Y (APPsw) cells produce more Aβ (58).

To investigate the effect of superoxide anion on the expression of UCP2 and UCP4, we examined the levels of these proteins after superoxide anion exposure and analyzed them

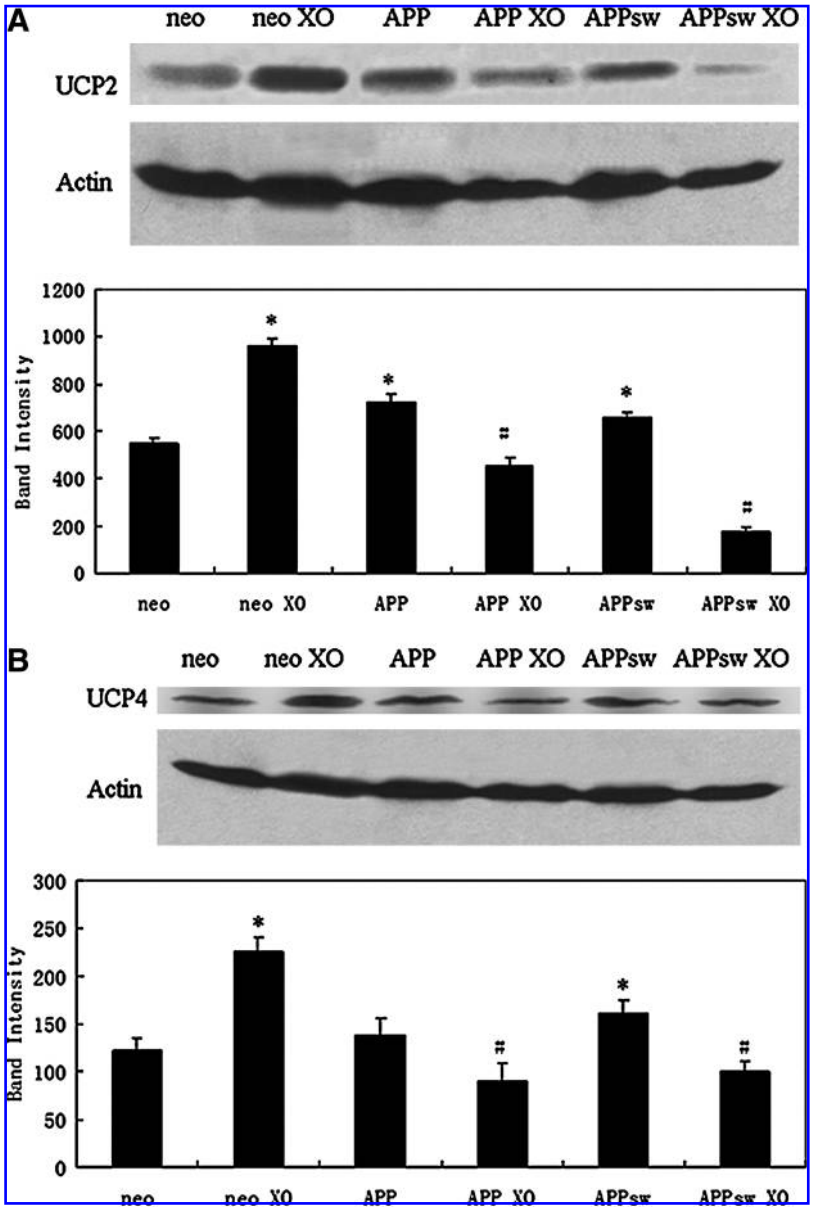

FIG. 1. Protein expressions of UCPs in the transgenic SH-SY5Y cells treated with superoxide anion and analyzed with Western blotting. (**A**) The UCP2 protein levels in the transgenic SH-SY5Y cell strains after incubating the cells with 50 m*M* xanthine plus xanthine oxidase (0.01 U per 3.5 ml) for 3 h. The lower panel is the statistical result of (**A**). (**B**) UCP4 protein levels with the same treatment. The lower panel is the statistical result of (**B**). The relative band intensity was standardized with the corresponding β-actin band intensity. $^*p < 0.05$ compared with neo; $\#p < 0.05$ compared with neo XO. The results are presented as mean ± SEM, $n = 4$. XO, treated with xanthine plus xanthine oxidase [40×60 mm (300×300 DPI)].

with Western blotting (Fig. 1). It was found that 3 h of treatment with superoxide anion, which was generated by xanthine plus xanthine oxidase (21), markedly changed the UCP2 and UCP4 protein levels in the SH-SY5Y cells. However, the results among the three cell strains differed markedly. The protein levels of UCP2 and UCP4 were both upregulated in SH-SY5Y (neo) but downregulated in SH-SY5Y (APP) and SH-SY5Y (APPsw) cell strains. The effectiveness of the superoxide anion production by xanthine plus xanthine oxidase is shown in supplemental Fig. 1 (see www.liebertonline.com/ars). We obtained similar results of UCP2 and UCP4 in the cells after knockdown of APP with siRNA and superoxide exposure (Fig. 2C and D).

Association of mitochondrial free Ca^{2+} with UCPs

Our data show that the alteration of the mitochondrial free Ca^{2+} level was closely associated with the levels of UCP2 and UCP4 proteins in APP and APPsw cells before and after superoxide anion exposure.

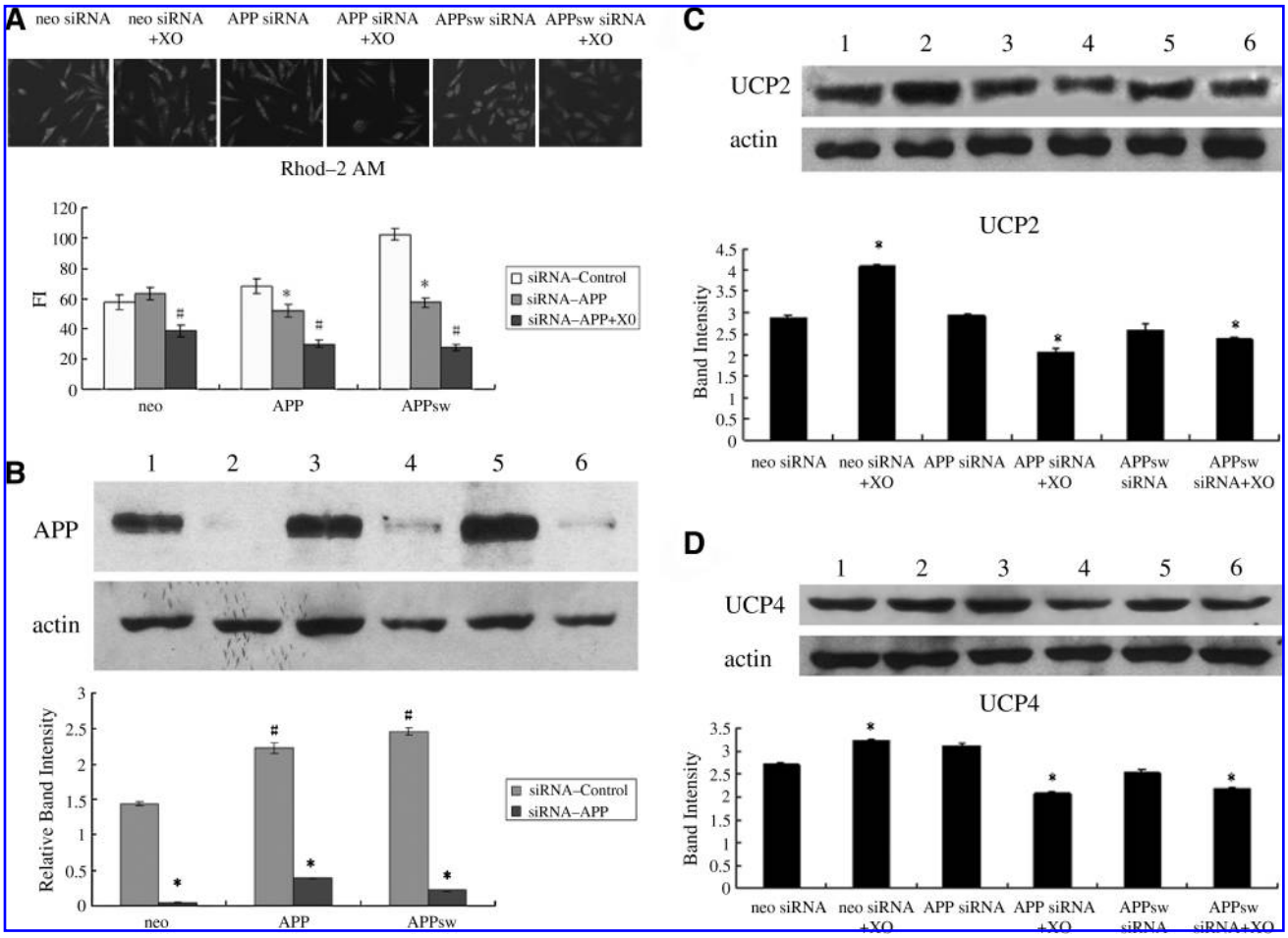

FIG. 2. (**A**) **Mitochondrial free Ca^{2+} levels after APP knockdown and superoxide exposure.** The upper panels show the typical live-cell images of the SH-SY5Y cells stained with rhod-2 AM under the fluorescence microscope (×200); each panel represents three independent experiments (siRNA control omitted for concision), and the lower panels show the statistical results of the mitochondrial free Ca^{2+} levels as presented in the upper panels. The mitochondrial free Ca^{2+} levels in the SH-SY5Y (APP) cells and the SH-SY5Y (APPsw) cells were significantly decreased after siRNA targeting APP for 24 h. Moreover, when the APP knockdown cells were exposed to 50 m*M* xanthine plus xanthine oxidase (0.01 U per 3.5 ml) for 3 h, the mitochondrial free Ca^{2+} levels all decreased significantly. The results are presented as mean ± SEM, $n = 30$. *$p < 0.05$ compared with the control; #$p < 0.05$ compared with the siRNA-APP. (**B**) Protein expressions of APP after APP knockdown in SH-SY5Y cells and the Western blotting analysis. The upper panels show the typical Western blotting results of APP before and after siRNA for 24 h. Lanes 1–6: neo siRNA control, neo siRNA, APP siRNA control, APP siRNA, APPsw siRNA control, and APPsw siRNA. (**C, D**) Protein expression of UCP2 and UCP4 in the SHSY5Y cells treated with siRNA against APP and superoxide. The upper panels show the typical Western blotting results of UCP2 and UCP4 after siRNA for 24 h and superoxide exposure for 3 h. Lanes 1–6: neo siRNA, neo siRNA + XO, APP siRNA, APP siRNA + XO, APPsw siRNA, and APPsw siRNA + XO. (**C**) Western blotting of UCP2. (**D**) Western blotting of UCP4. Whole-cell lysate containing 20 μg of total protein was loaded in each well. Each panel represents three independent experiments. The lower panels are the statistical results of the Western blotting represented by the upper panels. The relative band intensity was standardized with the corresponding β-actin band intensity. *$p < 0.05$ compared with control; #$p < 0.05$ compared with neo control. The results are presented as mean ± SEM, $n = 3$ [101×75 mm (300×300 DPI)].

Confocal microscopy of pericam-mt revealed that mitochondrial free Ca^{2+} levels shift, and these shifts in level are tightly coupled with the protein levels of UCP2 and UCP4 in the APP and APPsw overexpressed SH-SY5Y cells (Fig. 3). The pericam-mt fluorescence intensity is lower in SH-SY5Y (neo) cells than the values in SH-SY5Y (APP) and SH-SY5Y (APPsw) cells without superoxide exposure. Interestingly, the value of SH-SY5Y (APPsw) cells is the largest. However, the pericam-mt fluorescence intensity is the largest in SH-SY5Y (neo) cells after superoxide exposure among the cell strains. The values are obviously decreased in SH-SY5Y (APP) and SH-SY5Y (APPsw) cells after superoxide exposure. These results are consistent with the changes of UCP2 and UCP4 proteins among the SH-SY5Y cell strains.

Another selective fluorescent indicator for mitochondrial Ca^{2+}, rhod-2 AM, was also used to detect the mitochondrial free Ca^{2+} alteration. Similarly, the mitochondrial free Ca^{2+} alteration was heavily dependent on the protein levels of UCP2 and UCP4 (Fig. 4). Mitochondrial free Ca^{2+} levels expressed by the color fluorescence intensity scale of rhod-2 can be seen in supplemental Fig. 2 (see www.liebertonline.com/ars). The mitochondrial free Ca^{2+} decreased significantly (APP, −66.82%; $p < 0.001$; APPsw, −63.44%; $p < 0.001$) and increased in SH-SY5Y (neo) cells (30.26%; $p < 0.05$) after the cells were exposed to superoxide (Fig. 4A). To exclude possible false effects of our superoxide generation system, xanthine and inactivated xanthine oxidase were used; no significant difference was found between the control group and the treated group.

When UCP2 siRNA was introduced into the cell strains, the mitochondrial free Ca^{2+} levels, which were expressed by the fluorescence intensity of rhod-2, were decreased by 42.41% (neo; $p < 0.001$), 54.27% (APP; $p < 0.001$), and 63.30% (APPsw; $p < 0.001$), respectively (Fig. 4B). When UCP 4 siRNA was introduced into the cell strains, the mitochondrial free Ca^{2+} levels were decreased by 72.73% (neo; $p < 0.001$), 75.99% (APP; $p < 0.001$), and 77.69% (APPsw; $p < 0.001$), respectively (Fig. 4C). In addition, when UCP2 and UCP4 siRNAs were simultaneously introduced into the cell strains, larger decreases were observed (neo, −83.02%; $p < 0.001$; APP, −81.39%; $p < 0.001$; APPsw, −84.48%; $p < 0.001$) (Fig. 4D). Moreover, when the cells were treated with negative control siRNA followed with superoxide exposure, the mitochondrial free Ca^{2+} was decreased in the superoxide-treated group (Fig. 4E). In contrast, when the cells were treated with siRNA targeting UCP2 (Fig. 4F) or UCP4 (Fig. 4G) followed with superoxide exposure, we observed no significant difference between the control group and the superoxide-treated group.

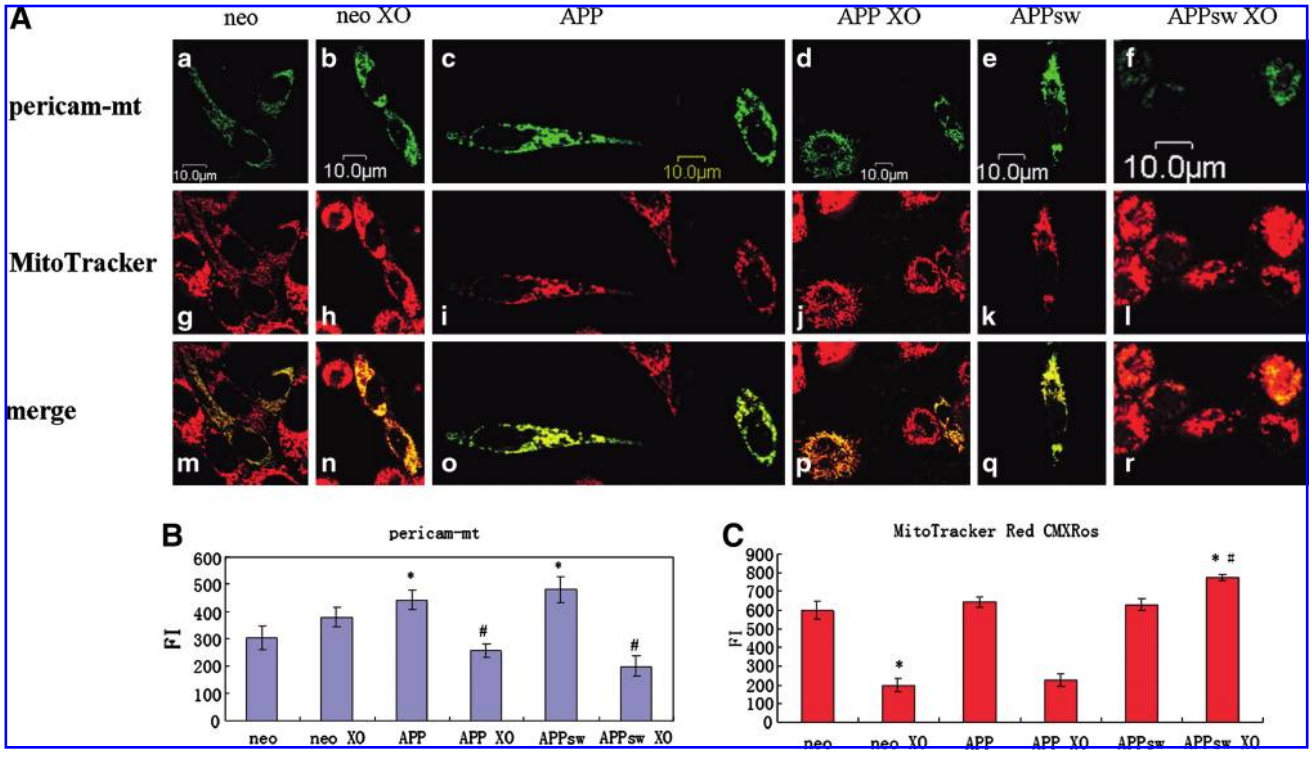

FIG. 3. (**A**) **Live-cell confocal images of the SH-SY5Y cells transiently transfected with the pericam-mt.** (**a–f**) The fluorescence images (green) of the pericam-mt in the cell strains before and after incubating the cells with 50 m*M* xanthine plus xanthine oxidase (0.01 U per 3.5 ml) for 3 h. (**g–l**) Fluorescence images (red) of MitoTracker Red CMXRos in the cell strains, which were incubated with 25 n*M* MitoTracker Red CMXRos for 40 min in growth medium before observation. (**m–r**) Merged fluorescence images (yellow) of the pericam-mt and MitoTracker Red CMXRos. (**B**) Statistical result of the pericam-mt as presented in (**A**). *$p < 0.05$ compared with neo; #$p < 0.05$ compared with neo XO. The results are presented as mean ± SEM, $n = 10$. FI, fluorescence intensity. (**C**) Statistical result of the mitochondrial membrane potential (represented by MitoTracker Red CMXRos as presented in (**A**). *$p < 0.05$ compared with neo; #$p < 0.05$ compared with neo XO. The results are presented as mean ± SEM, $n = 16$ [150×91 mm (300×300 DPI)]. (For interpretation of the references to color in this figure legend, the reader is referred to the web version of this article at www.liebertonline.com/ars).

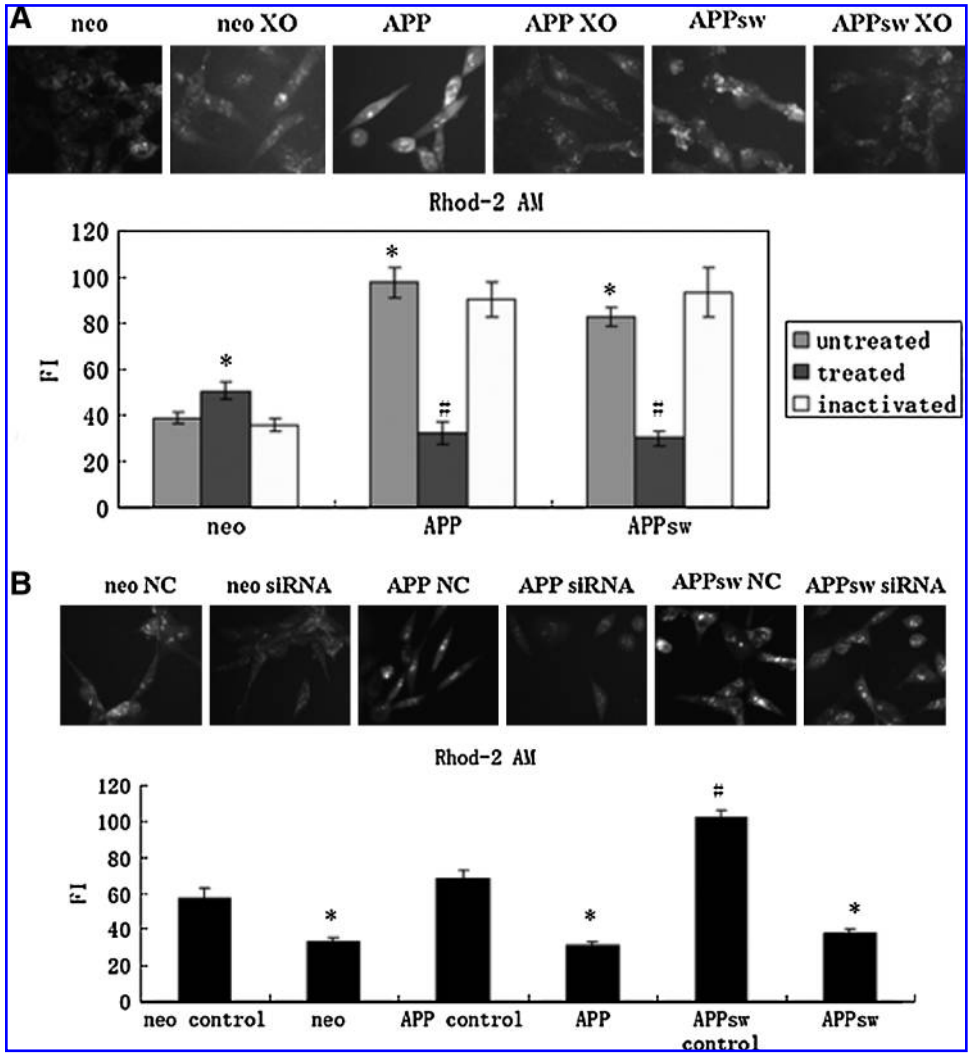

FIG. 4. Mitochondrial free Ca^{2+} levels expressed by the fluorescence intensity of rhod-2. (**A–G**) The upper panels show the typical live-cell images of the transgenic SH-SY5Y cell strains stained with rhod-2 AM under the fluorescence microscope (×200); each panel represents three independent experiments, and the lower panels show the statistical results of the mitochondrial free Ca^{2+} levels as presented in the upper panels. NC, treated with negative control siRNA. (**A**) The mitochondrial free Ca^{2+} levels in the SH-SY5Y cells after incubating the cells with 50 m*M* xanthine plus xanthine oxidase (0.01 U per 3.5 ml) for 3 h (treated) or with 50 m*M* xanthine plus xanthine oxidase (0.01 U per 3.5 ml heated at 100°) for 3 h (inactivated). $^*p < 0.05$ compared with neo (untreated); $\#p < 0.05$ compared with neo (treated). (**B**) The mitochondrial free Ca^{2+} levels in the SH-SY5Y cells after siRNA targeting UCP2. $^*p < 0.05$ compared with control; $\#p < 0.05$ compared with neo control.

Figure 5 shows the UCP2 and UCP4 siRNA efficiency. These results confirm the findings of confocal microscopy by transiently transfecting the pericam-mt.

APP knockdown reversed the differences of the mitochondrial free Ca^{2+} levels among the transgenic SH-SY5Y cell strains

As shown in Fig. 2A, the mitochondrial free Ca^{2+} levels were significantly downregulated by APP knockdown in SH-SY5Y (APP) cells and SH-SY5Y (APPsw) cells; this differs from that found in the UCPs siRNA experiment (Fig. 4F and G). The Western blot confirmed the APP knockdown effect (Fig. 2B).

Mitochondrial membrane potentials were changed after superoxide exposure in the SH-SY5Y cell strains

Mitochondrial membrane potential is an important indicator for cell death, the aging process, and mitochondrial function. To measure mitochondrial membrane potential, we stained the cells with MitoTracker Red CMXRos, a potential-dependent fluorescent probe specific for mitochondria. The relative changes in fluorescence intensity were −67.17% and −65.01% in SH-SY5Y (neo) cells and SH-SY5Y (APP) cells, compared with the untreated cells (Fig. 3C). However, no significant change occurred in SH-SY5Y (APPsw) cells with or without superoxide exposure. The reduction of mitochondrial membrane potential induced by superoxide anion is one kind of protective mechanism, by which the decreasing mitochondrial membrane potential can reduce superoxide anion generation to avoid extra mitochondrial damage and dysfunction due to the excessive superoxide in cells (2, 6, 8, 20). However, this protective feedback seems to be disrupted in SH-SY5Y (APPsw) cells because of the expression of APP-Swedish mutation.

Mitochondrial free Ca^{2+} levels were independent of the mitochondrial membrane potentials

By simultaneous detection of the fluorescence intensities of the pericam-mt and MitoTracker Red CMXRos with a confocal microscope, we found no linear correlation between the mitochondrial free Ca^{2+} levels and the mitochondrial membrane potentials in our cell models (Fig. 3B and C).

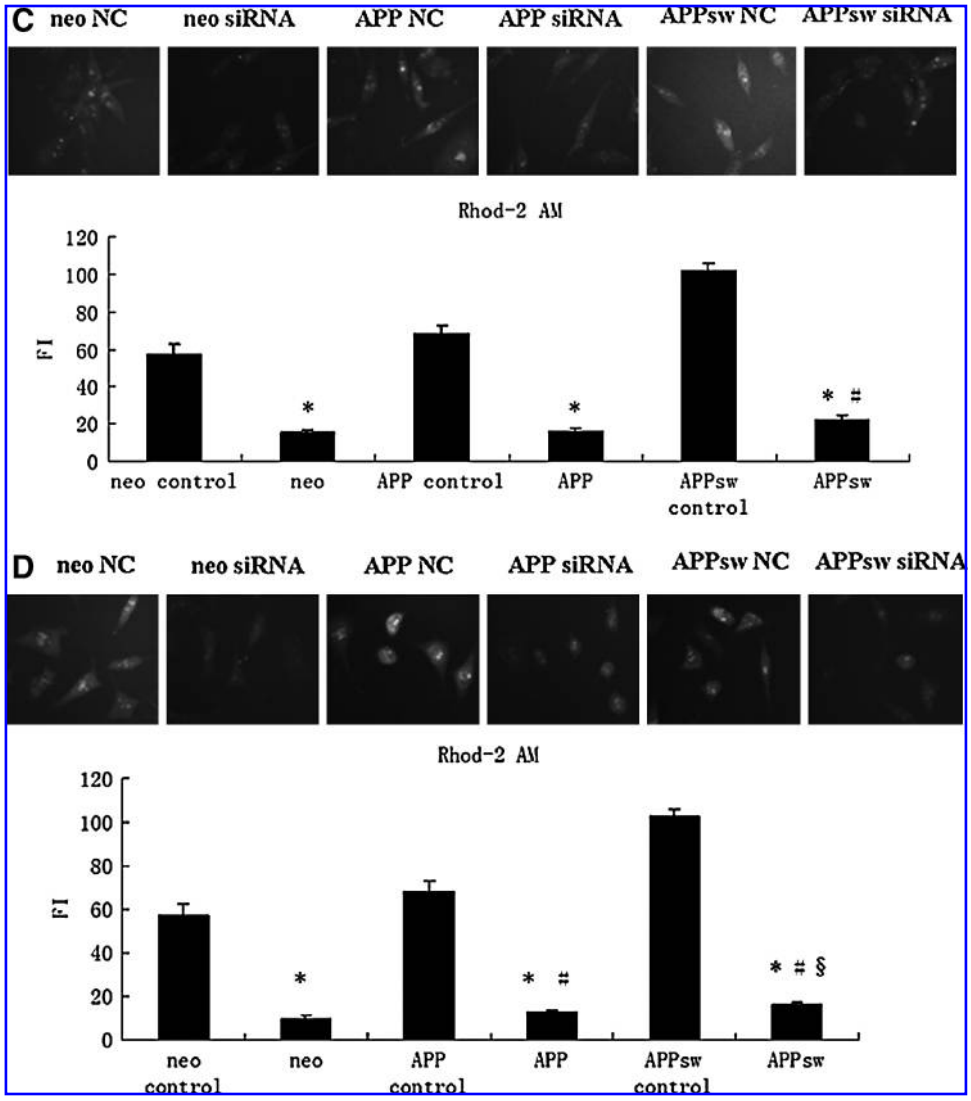

FIG. 4. *Continued*. (**C**) Mitochondrial free Ca^{2+} levels in the SH-SY5Y cells after siRNA targeting UCP4. $*p < 0.05$ com-0.05 compared with control; $\#p < 0.05$ compared with neo. (**D**) The mitochondrial free Ca^{2+} levels in the SH-SY5Y cells after siRNA targeting UCP2 and UCP4. $*p < 0.05$ compared with control; $\#p < 0.05$ compared with neo; $\S p < 0.05$ compared with APP.

Deficiency of mitochondrial free Ca^{2+} levels in the response to histamine after superoxide exposure in SH-SY5Y (APP) and SH-SY5Y (APPsw) cells

To determine functional effects of altered UCPs levels on mitochondrial Ca^{2+} carrier function in the cells, we monitored changes in the fluorescence intensity of rhod-2 after histamine administration to the cell strains. Histamine is an agonist of cytosolic Ca^{2+}, which induces cytosolic Ca^{2+} elevation through inducing endoplasmic reticulum Ca^{2+} release. In the control group, the mitochondrial free Ca^{2+} concentration is lower in SH-SY5Y (neo) cells than in SH-SY5Y (APP) and SH-SY5Y (APPsw) cells before histamine administration. After histamine administration, the mitochondrial free Ca^{2+} concentration significantly increased in SH-SY5Y (neo) cells but decreased in SH-SY5Y (APP) and SH-SY5Y (APPsw) cells (Fig. 6A). In the treated group, with 50 m*M* xanthine plus xanthine oxidase (0.01 U per 3.5 ml) for 3 h, the mitochondrial free Ca^{2+} concentrations were equally low in the cells before histamine administration. SH-SY5Y (neo) cells showed more of an increase in the mitochondrial free Ca^{2+} concentration than in SH-SY5Y (APP) and SH-SY5Y (APPsw) cells after histamine administration (Fig. 6B). Obviously, the ability of the mitochondrial free Ca^{2+} level responding to histamine after superoxide exposure in SH-SY5Y (APP) and SH-SY5Y (APPsw) cells is deficient.

PPAR-γ plays a key role in the pathway of UCPs regulation by superoxide

Western-blotting analysis of PPAR-γ shows coherent changes with UCP2 and UCP4 in the three cell strains (Fig. 7). However, the situation seemed complicated after superoxide exposure; we found that UCPs decreased, whereas PPAR-γ did not change significantly in SH-SY5Y (APP) cells after superoxide exposure. Interestingly, after superoxide exposure, the change of PPAR-γ in SH-SY5Y (APP) cells is just a transition state between the changes of PPAR-γ in SH-SY5Y (neo) cells and SH-SY5Y (APPsw) cells.

Discussion

Accumulating evidence shows that UCPs play a major role in mediating proton leak to cause mild uncoupling,

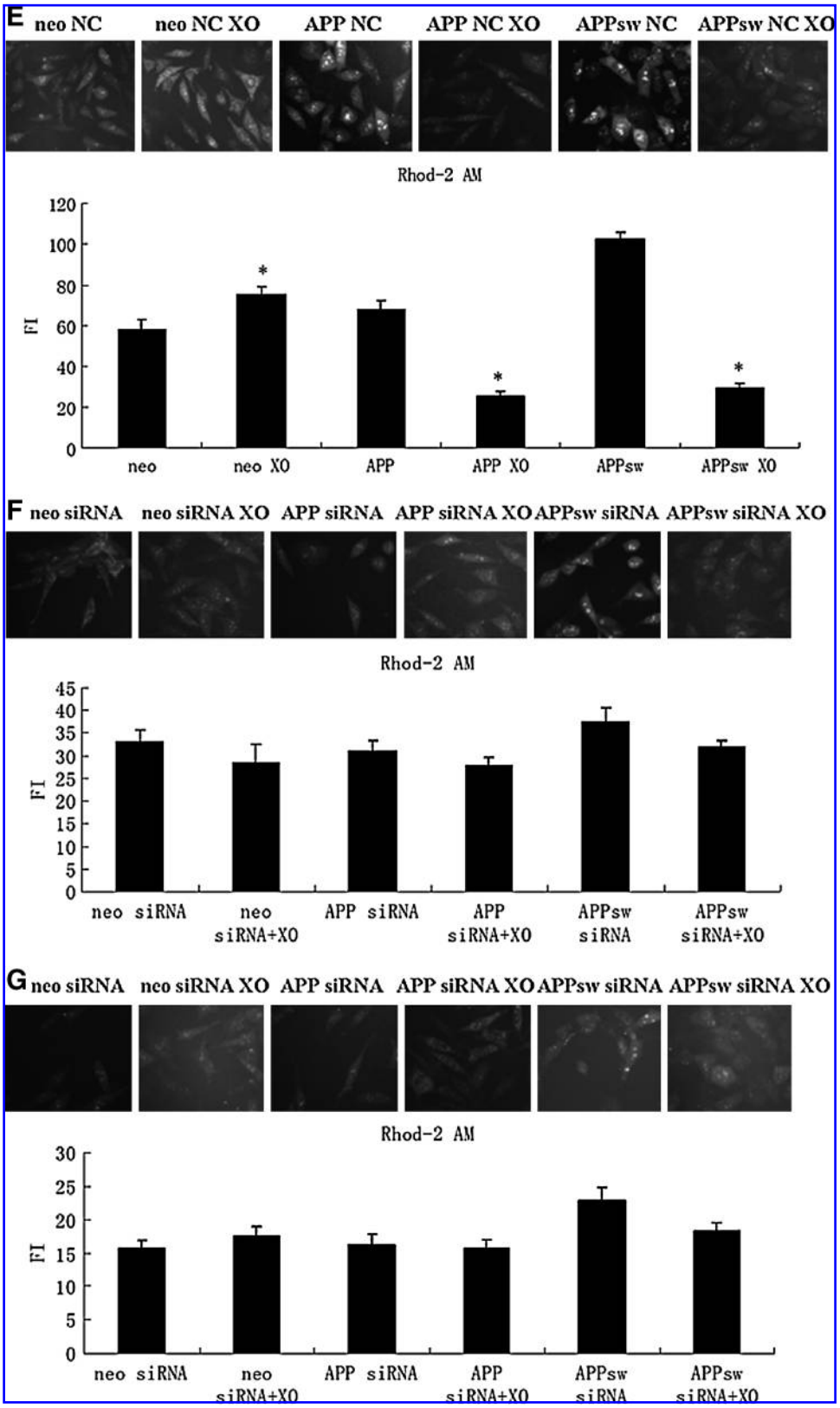

FIG. 4. *Continued*. (**E**) The mitochondrial free Ca^{2+} levels in the SHSY5Y cells after treatment with negative control siRNA for 24 h and 50 m*M* xanthine plus xanthine oxidase (0.01 U per 3.5 ml) for 3 h. *$p < 0.05$ compared with control. (**F**) The mitochondrial free Ca^{2+} levels in the SHSY5Y cells after treatment with siRNA targeting UCP2 for 24 h and 50 m*M* xanthine plus xanthine oxidase (0.01 U per 3.5 ml) for 3 h. (**G**) The mitochondrial free Ca^{2+} levels in the SHSY-5Y cells after treatment with siRNA targeting UCP4 for 24 h and 50 m*M* xanthine plus xanthine oxidase (0.01 U per 3.5 ml) for 3 h. The results are presented as mean ± SEM, $n = 30$ [150× 194 mm (300×300DPI)].

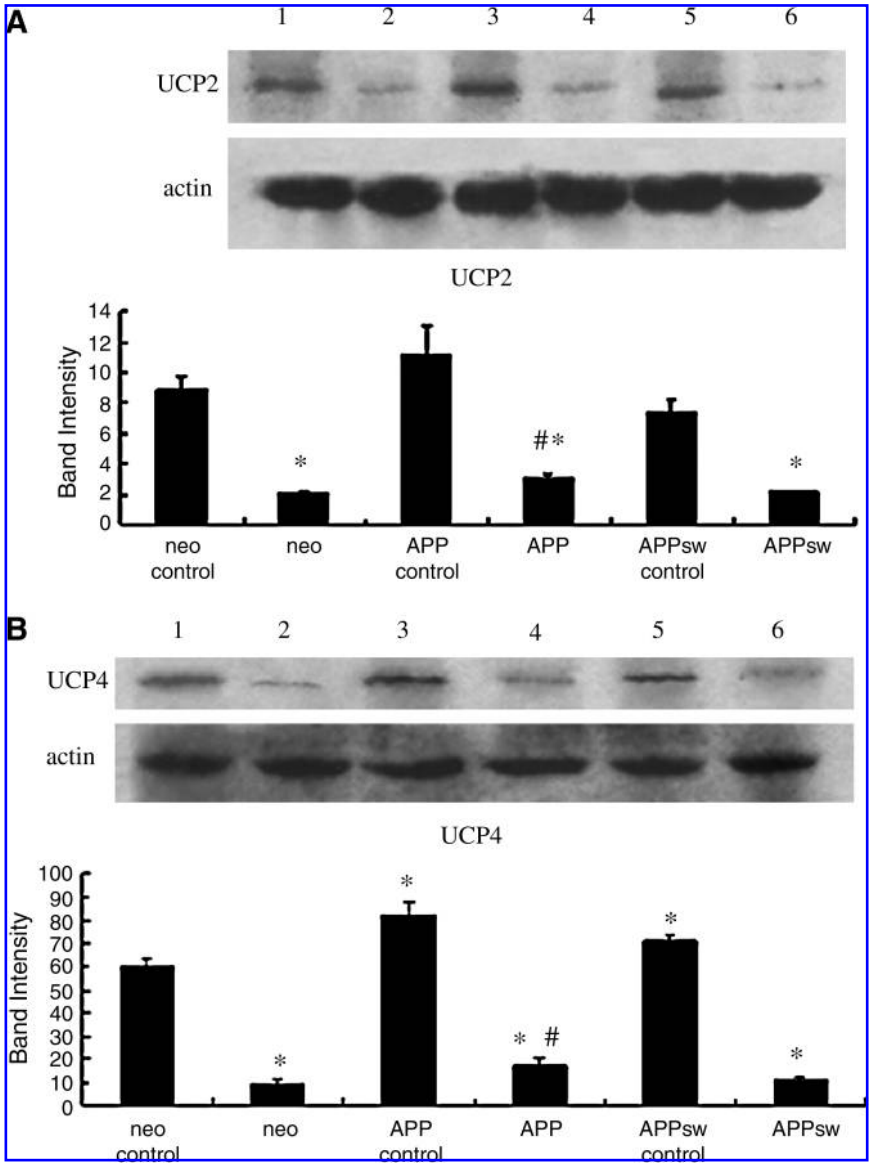

FIG. 5. Protein expression of UCP2 and UCP4 in the SH-SY5Y cells treated with siRNA and the Western blotting analysis. (**Upper panels**) Typical Western blotting results of UCP2 and UCP4 after siRNA for 24 h. Whole-cell lysate containing 20 μg of total protein was loaded in each well. Each panel represents three independent experiments. Lanes 1–6: neo siRNA control, neo siRNA, APP siRNA control, APP siRNA, APPsw siRNA control, and APPsw siRNA. (**Lower panels**) The statistical results of the Western blotting results represented by the upper panels. (**A**) Western blotting of UCP2; (**B**) Western blotting of UCP4. The relative band intensity was standardized with the corresponding β-actin band intensity. $^*p < 0.05$ compared with neo control; $\#p < 0.05$ compared with neo. The results are presented as mean $\pm$ SEM, $n = 3$ [46×72 mm (300×300 DPI)].

diminishing the production of mitochondrial superoxide anion, and protecting against oxidative damage or causing increased thermogenesis (4, 5, 7, 11, 20, 28, 40). Several recent reports suggested that UCPs are involved in mitochondrial Ca^{2+} homeostasis as Ca^{2+} carriers (12, 52). With the ROBETTA full-chain protein structure prediction server (http://robetta.bakerlab.org), the protein structure of UCPs was predicted to form a channel-like structure, and the protonated A-R-E-E domain of UCPs in the second intermembrane loop was suggested to be the domain that is crucial for the Ca^{2+} conductance of UCPs (52). Our results support a mitochondrial Ca^{2+}-carrier role for UCPs.

Previous studies put an emphasis on the effects of UCPs in decreasing mitochondrial superoxide. Our results show that the superoxide anion increased UCP2 and UCP4 protein levels in SH-SY5Y (neo) cells, but decreased UCP2 and UCP4 protein levels in SH-SY5Y (APP) and SH-SY5Y (APPsw) cells, which represent cells overexpressing APP and cells with an AD causing mutated APP in our models, respectively. Superoxide was added to the cells to imitate the oxidative-stress environment in an AD brain. Notably, the susceptibilities of the cells with different APP forms in response to superoxide anion were entirely different. In SH-SY5Y (neo) cells, which express endogenous APP, the mitochondrial Ca^{2+} concentration was significantly increased after superoxide exposure.

In contrast, in SH-SY5Y (APP) and SH-SY5Y (APPsw) cells, which express excessive APP or mutated APP, the mitochondrial Ca^{2+} concentration was significantly decreased after superoxide exposure. This result shows that APP or its derivative (most probably, β-amyloid) could affect the susceptibility of the cell to oxidative stress. Consistent with our finding, the protein levels of UCP2, UCP4, and UCP5 were significantly reduced in AD brains (15). The changes in mitochondrial free Ca^{2+} level were tightly correlated with the protein levels of UCP2 and UCP4 in SH-SY5Y (APP) and SH-SY5Y (APPsw) cells. Our siRNA results further support that UCP2 and UCP4 both play important roles in mitochondrial Ca^{2+} homeostasis. The mitochondrial function of Ca^{2+} regulation will be impaired by decreased levels of UCP2 and

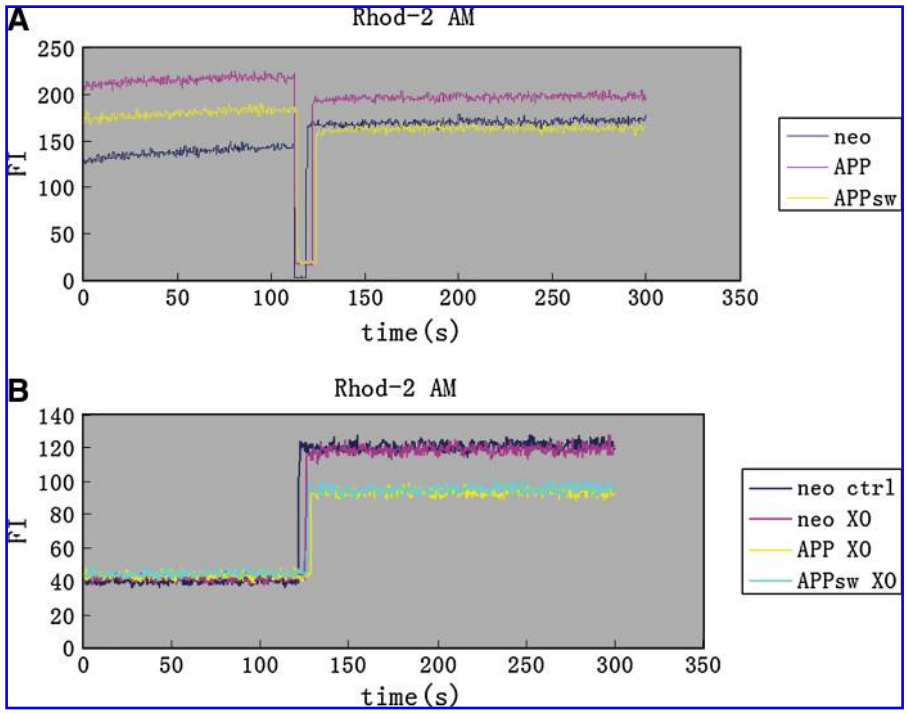

FIG. 6. Mitochondrial free Ca^{2+} levels in the response to histamine after superoxide exposure in the SH-SY5Y cells. (**A**) Typical responses of the untreated cells. The lines represent the time-lapse of the mitochondrial free Ca^{2+} levels in the response to histamine in the SH-SY5Y cells. Blue line, the SH-SY5Y (neo) cells; purple line, the SH-SY5Y (APP) cells; yellow line, the SH-SY5Y (APPsw) cells. (**B**) Typical responses of the cells preincubated with 50 m*M* xanthine plus xanthine oxidase (0.01 U per 3.5 ml) for 3 h. Blue line, the SH-SY5Y (neo) cells; purple line, the SH-SY5Y (neo) cells preincubated with XO; yellow line, the SH-SY5Y (APP) cells preincubated with XO; light blue line, the SH-SY5Y (APPsw) cells preincubated with XO. The cells were counted before detection to make a cell suspension of 1×10 6/ml, and 100 μM histamine was mixed into the cell suspension at 2 min after the beginning of detection. The mitochondrial free Ca^{2+} levels are expressed by the fluorescence intensity of rhod-2. Each line represents three independent experiments [150×135 mm (300×300 DPI)]. (For interpretation of the references to color in this figure legend, the reader is referred to the web version of this article at www.liebertonline.com/ars).

UCP4, and this will subsequently lead to disturbances in Ca^{2+} signaling, intracellular Ca^{2+} overload, and apoptosis. Furthermore, UCP4 is a more possible potential target than is UCP2 in AD treatment, because UCP4 is specifically expressed in neuronal cells (43). Supporting for this view, our results suggest UCP4 played a larger role in mitochondrial Ca^{2+} homeostasis than did UCP2.

Important in calcium storage, mitochondria have a large capacity for calcium uptake. Except for UCPs, another factor that can affect intramitochondrial Ca^{2+} concentration is the

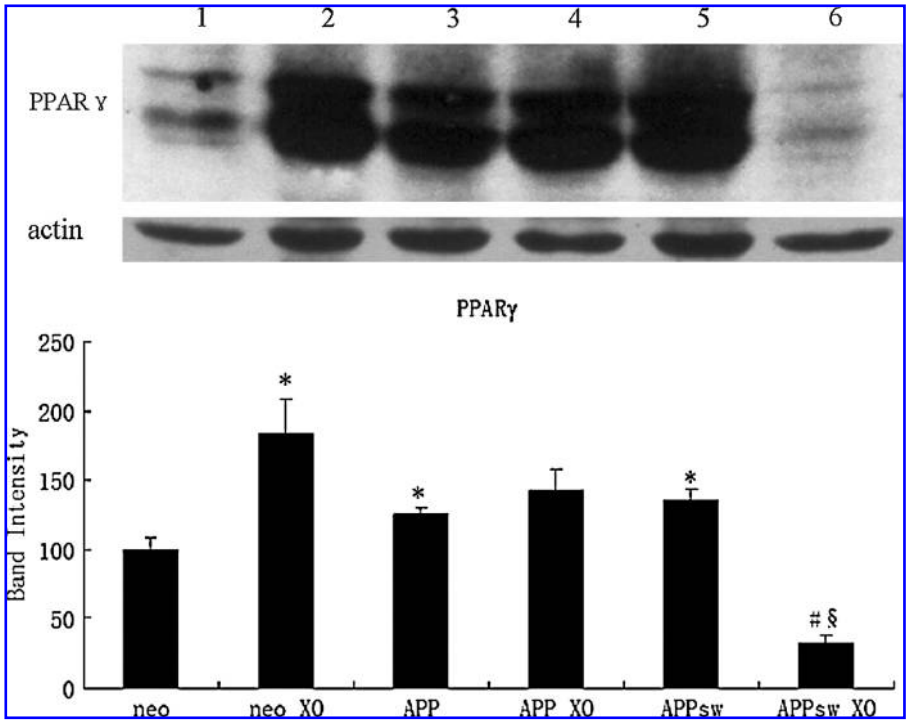

FIG. 7. Protein expression of PPAR-γ in the SH-SY5Y cells treated with superoxide. The upper panel shows the typical Western blotting results of PPAR-γ after superoxide exposure for 3 h. Whole-cell lysate containing 20 μg of total protein was loaded in each well. Lanes 1–6: neo, neo + XO, APP, APP + XO, APPsw, and APPsw + XO. The lower panel is the statistical results of the Western blotting represented by the upper panel. The relative band intensity was standardized with the corresponding β-actin band intensity. *$p < 0.05$ compared with neo; #$p < 0.05$ compared with neo XO; §$p < 0.05$ compared with respective control. The results are presented as mean ± SEM, $n = 3$ [50×42mm (300×300 DPI)].

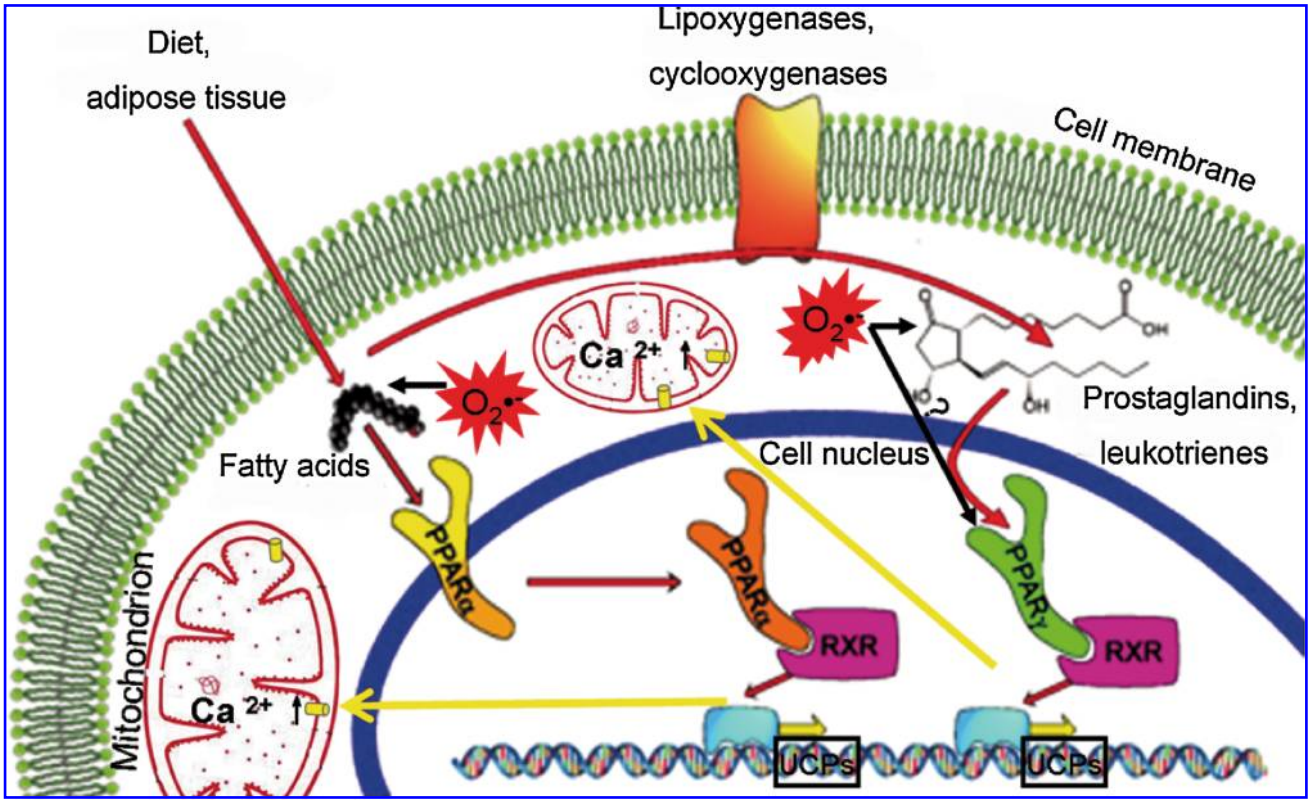

FIG. 8. Schematic representation of the proposed pathway of mitochondrial Ca^{2+} regulated by superoxide through UCPs. Superoxide affects PPAR-γ activation through acting with PPAR-γ ligands or PPAR-γ directly. After ligand activation, PPAR-γ forms a heterodimer with retinoid X receptor (RXR) and binds to the promoter domain of target genes. Subsequent expression of UCPs leads to an increase of mitochondrial free Ca^{2+}. Yellow, UCPs embedded in the mitochondrial inner membrane [75×45 mm (300×300 DPI)]. (For interpretation of the references to color in this figure legend, the reader is referred to the web version of this article at www.liebertonline.com/ars).

inner mitochondrial membrane potential (41, 50). A previous viewpoint is that the ability of neuronal UCPs to regulate the mitochondrial membrane potential underlies their ability to regulate neuronal calcium homeostasis (2). However, our results on mitochondrial membrane potential obviously indicate another pathway by which UCPs regulate neuronal calcium homeostasis, independent of mitochondrial membrane potential. The situation is interesting because the mitochondrial Ca^{2+} concentration was slightly increased after superoxide exposure, whereas the mitochondrial membrane potential was significantly decreased in SH-SY5Y (neo) cells. In contrast, the mitochondrial Ca^{2+} concentration was significantly decreased after superoxide exposure, whereas the mitochondrial membrane potential was significantly increased in SH-SY5Y (APPsw) cells (Fig. 3C). Only in SH-SY5Y (APP) cells did the mitochondrial Ca^{2+} concentration and the mitochondrial membrane potential decrease coordinately. In our cell models, these findings show that mitochondrial membrane potential is not the main factor by which UCPs regulate mitochondrial calcium homeostasis.

Moreover, quite a few articles support protective roles of UCPs for neurons and other types of cells (16–18, 26, 31, 32, 35, 54, 59, 60). On the mechanisms of how UCPs can perform the protective roles for cells, most explanations assume that UCPs can attenuate oxidative stress. As considerable evidence suggests a positive signaling role for superoxide anion, which is the primary free radical of oxidative stress, we have reason to think that it is not the right answer (36, 46, 55, 56). Although further work should be carried out on animal models and human subjects, the protective roles of UCPs and their mechanisms may be relevant to AD.

The PPAR-γ levels in postmortem brain sections from AD patients have been examined. They showed 40% reductions in PPAR-γ protein levels in AD patients compared with controls. Moreover, PPAR-γ has been found to disappear in senile plaques. PPAR-γ was indicated to be involved in the modulation of the amyloid cascade, causing AD (42, 45); conversely, PPAR-γ was suggested to be a key regulator of UCPs (53). Taken together, this linkage implies potential pathways between UCPs and the amyloid cascade. Our findings suggest such a pathway by which UCPs are possibly involved in the pathogenesis of AD. Here, based on previous studies and our research, we propose a pathway of mitochondrial Ca^{2+} regulated by superoxide through UCPs in a schematic representation (Fig. 8). Under the condition of oxidative stress, increased superoxide may affect PPAR-γ activation through acting with PPAR-γ ligands or PPAR-γ directly. After ligand activation, PPAR-γ forms a heterodimer with retinoid X receptor (RXR) and binds to the promoter domain of target genes. Subsequent expression and translocation of UCPs leads to an increase of mitochondrial free Ca^{2+}. This pathway may be disrupted at several points, and the disrupted point is the expression of PPAR-γ, which was weakened in our cell models (Fig. 7). In line with this pathway, an article suggests

that ghrelin can increase mitochondrial fatty acid beta oxidation through UCP2 (3).

Given the remarkably strong effects of UCP2 and UCP4 on the mitochondrial free Ca^{2+} sequestration in the SH-SY5Y cells demonstrated thus far, we may be cautiously optimistic that pharmacologic modulation of UCPs will become a viable therapeutic approach for AD and possibly for other neurodegenerative diseases as well.

Acknowledgments

We thank Dr. Yan Teng for assistance on confocal microscopy. We thank Dr. Atsushi Miyawaki (Laboratory for Cell Function and Dynamics, Advanced Technology Development Center, Brain Science Institute, RIKEN, Saitama, Japan) for kindly providing us the ratiometric-pericam-mt. We thank Prof. Heping Cheng (Peking University, China) for the mito-cpYFP plasmid. This work was supported by a grant from the National Natural Science Foundation of China (30370361) and 973 grant (2006CB500700). This research was partly supported by Key Laboratory of Mental Health, Chinese Academy of Sciences. It was supported in part by E-Institutes of Shanghai Municipal Education Commission, Project Number: E-04010.

Abbreviations

AD, Alzheimer's disease; APP, β-amyloid precursor protein; APPsw, β-amyloid precursor protein Swedish mutation; BCA, bicinchoninic acid; BMCP1, brain mitochondrial carrier protein-1; $[Ca^{2+}]_{mito}$, mitochondrial free Ca^{2+} concentration; DMEM, Dulbecco's modified Eagle's medium; ECL, enhanced chemiluminescence; FI, fluorescence intensity; HRP, horseradish peroxidase; pericam-mt, mitochondria-targeted ratiometric-pericam; rhod-2 AM, rhod-2 acetoxymethyl ester; ROS, reactive oxygen species; SDS–PAGE, sodium dodecyl sulfate–polyacrylamide gel electrophoresis; TBS-T, Tris-buffered saline with 0.1% Tween 20; XO, xanthine oxidase; UCPs, uncoupling proteins.

Author Disclosure Statement

No competing financial interests exist.

References

1. Ambrose M, Goldstine JV, and Gatti RA. Intrinsic mitochondrial dysfunction in ATM-deficient lymphoblastoid cells. *Hum Mol Genet* 16: 2154–2164, 2007.
2. Andrews ZB, Diano S, and Horvath TL. Mitochondrial uncoupling proteins in the CNS: in support of function and survival. *Nat Rev Neurosci* 6: 829–840, 2005.
3. Andrews ZB, Liu ZW, Walllingford N, Erion DM, Borok E, Friedman JM, Tschop MH, Shanabrough M, Cline G, Shulman GI, Coppola A, Gao XB, Horvath TL, and Diano S. UCP2 mediates ghrelin's action on NPY/AgRP neurons by lowering free radicals. *Nature* 454: 846–851, 2008.
4. Arsenijevic D, Onuma H, Pecqueur C, Raimbault S, Manning BS, Miroux B, Couplan E, Alves-Guerra MC, Goubern M, Surwit R, Bouillaud F, Richard D, Collins S, and Ricquier D. Disruption of the uncoupling protein-2 gene in mice reveals a role in immunity and reactive oxygen species production. *Nat Genet* 26: 435–439, 2000.
5. Brand MD, Affourtit C, Esteves TC, Green K, Lambert AJ, Miwa S, Pakay JL, and Parker N. Mitochondrial superoxide: production, biological effects, and activation of uncoupling proteins. *Free Radic Biol Med* 37: 755–767, 2004.
6. Brand MD and Esteves TC. Physiological functions of the mitochondrial uncoupling proteins UCP2 and UCP3. *Cell Metab* 2: 85–93, 2005.
7. Brand MD, Pamplona R, Portero-Otin M, Requena JR, Roebuck SJ, Buckingham JA, Clapham JC, and Cadenas S. Oxidative damage and phospholipid fatty acyl composition in skeletal muscle mitochondria from mice underexpressing or overexpressing uncoupling protein 3. *Biochem J* 368: 597–603, 2002.
8. Brookes PS, Yoon Y, Robotham JL, Anders MW, and Sheu SS. Calcium, ATP, and ROS: a mitochondrial love-hate triangle. *Am J Physiol* 287: C817–C833, 2004.
9. Butterfield DA, Reed T, Newman SF, and Sultana R. Roles of amyloid beta-peptide-associated oxidative stress and brain protein modifications in the pathogenesis of Alzheimer's disease and mild cognitive impairment. *Free Radic Biol Med* 43: 658–677, 2007.
10. Camello-Almaraz C, Gomez-Pinilla PJ, Pozo MJ, and Camello PJ. Mitochondrial reactive oxygen species and Ca^{2+} signaling. *Am J Physiol* 291: C1082–C1088, 2006.
11. Carafoli E. Historical review: mitochondria and calcium: ups and downs of an unusual relationship. *Trends Biochem Sci* 28: 175–181, 2003.
12. Chan SL, Liu D, Kyriazis GA, Bagsiyao P, Ouyang X, and Mattson MP. Mitochondrial uncoupling protein-4 regulates calcium homeostasis and sensitivity to store depletion-induced apoptosis in neural cells. *J Biol Chem* 281: 37391–37403, 2006.
13. Colvin RA, Bennett JW, Colvin SL, Allen RA, Martinez J, and Miner GD. Na^+/Ca^{2+} exchange activity is increased in Alzheimer's disease brain tissues. *Brain Res* 543: 139–147, 1991.
14. Cutler RG, Kelly J, Storie K, Pedersen WA, Tammara A, Hatanpaa K, Troncoso JC, and Mattson MP. Involvement of oxidative stress-induced abnormalities in ceramide and cholesterol metabolism in brain aging and Alzheimer's disease. *Proc Natl Acad Sci U S A* 101: 2070–2075, 2004.
15. de la Monte SM and Wands JR. Molecular indices of oxidative stress and mitochondrial dysfunction occur early and often progress with severity of Alzheimer's disease. *J Alzheimers Dis* 9: 167–181, 2006.
16. Degasperi GR, Romanatto T, Denis RG, Araujo EP, Moraes JC, Inada NM, Vercesi AE, and Velloso LA. UCP2 protects hypothalamic cells from TNF-alpha-induced damage. *FEBS Lett* 582: 3103–3110, 2008.
17. Deierborg T, Wieloch T, Diano S, Warden CH, Horvath TL, and Mattiasson G. Overexpression of UCP2 protects thalamic neurons following global ischemia in the mouse. *J Cereb Blood Flow Metab* 28: 1186–1195, 2008.
18. Derdak Z, Mark NM, Beldi G, Robson SC, Wands JR, and Baffy G. The mitochondrial uncoupling protein-2 promotes chemoresistance in cancer cells. *Cancer Res* 68: 2813–2819, 2008.
19. Duchen MR. Mitochondria and Ca(2+) in cell physiology and pathophysiology. *Cell Calcium* 28: 339–348, 2000.
20. Echtay KS. Mitochondrial uncoupling proteins: what is their physiological role? *Free Radic Biol Med* 43: 1351–1371, 2007.
21. Echtay KS, Roussel D, St-Pierre J, Jekabsons MB, Cadenas S, Stuart JA, Harper JA, Roebuck SJ, Morrison A, Pickering S, Clapham JC, and Brand MD. Superoxide activates mitochondrial uncoupling proteins. *Nature* 415: 96–99, 2002.
22. Feng X, Zhao P, He Y, and Zuo Z. Allele-specific silencing of Alzheimer's disease genes: the amyloid precursor protein

genes with Swedish or London mutations. *Gene* 371: 68–74, 2006.
23. Franchini M, Gandini G, de Gironcoli M, Vassanelli A, Borgna-Pignatti C, and Aprili G. Safety and efficacy of subcutaneous bolus injection of deferoxamine in adult patients with iron overload. *Blood* 95: 2776–2779, 2000.
24. Gunter TE, Yule DI, Gunter KK, Eliseev RA, and Salter JD. Calcium and mitochondria. *FEBS Lett* 567: 96–102, 2004.
25. Kim-Han JS and Dugan LL. Mitochondrial uncoupling proteins in the central nervous system. *Antioxid Redox Signal* 7: 1173–1181, 2005.
26. Kim JE, Kim YW, Lee IK, Kim JY, Kang YJ, and Park SY. AMP-activated protein kinase activation by 5-aminoimidazole-4-carboxamide-1-beta-D-ribofuranoside (AICAR) inhibits palmitate-induced endothelial cell apoptosis through reactive oxygen species suppression. *J Pharmacol Sci* 106: 394–403, 2008.
27. Kirichok Y, Krapivinsky G, and Clapham DE. The mitochondrial calcium uniporter is a highly selective ion channel. *Nature* 427: 360–364, 2004.
28. Klingenberg M and Echtay KS. Uncoupling proteins: the issues from a biochemist point of view. *Biochim Biophys Acta* 1504: 128–143, 2001.
29. Krauss S, Zhang CY, and Lowell BB. The mitochondrial uncoupling-protein homologues. *Nat Rev* 6: 248–261, 2005.
30. Krauss S, Zhang CY, Scorrano L, Dalgaard LT, St-Pierre J, Grey ST, and Lowell BB. Superoxide-mediated activation of uncoupling protein 2 causes pancreatic beta cell dysfunction. *J Clin Invest* 112: 1831–1842, 2003.
31. Lindholm D, Eriksson O, and Korhonen L. Mitochondrial proteins in neuronal degeneration. *Biochem Biophys Res Commun* 321: 753–758, 2004.
32. Liu D, Chan SL, de Souza-Pinto NC, Slevin JR, Wersto RP, Zhan M, Mustafa K, de Cabo R, and Mattson MP. Mitochondrial UCP4 mediates an adaptive shift in energy metabolism and increases the resistance of neurons to metabolic and oxidative stress. *Neuromol Med* 8: 389–414, 2006.
33. Lopez JR, Lyckman A, Oddo S, Laferla FM, Querfurth HW, and Shtifman A. Increased intraneuronal resting [Ca2+] in adult Alzheimer's disease mice. *J Neurochem* 105: 262–271, 2008.
34. Malli R, Frieden M, Trenker M, and Graier WF. The role of mitochondria for Ca^{2+} refilling of the endoplasmic reticulum. *J Biol Chem* 280: 12114–12122, 2005.
35. Mattiasson G, Shamloo M, Gido G, Mathi K, Tomasevic G, Yi S, Warden CH, Castilho RF, Melcher T, Gonzalez-Zulueta M, Nikolich K, and Wieloch T. Uncoupling protein-2 prevents neuronal death and diminishes brain dysfunction after stroke and brain trauma. *Nat Med* 9: 1062–1068, 2003.
36. Mouche S, Mkaddem SB, Wang W, Katic M, Tseng YH, Carnesecchi S, Steger K, Foti M, Meier CA, Muzzin P, Kahn CR, Ogier-Denis E, and Szanto I. Reduced expression of the NADPH oxidase NOX4 is a hallmark of adipocyte differentiation. *Biochim Biophys Acta* 1773: 1015–1027, 2007.
37. Multhaup G, Scheuermann S, Schlicksupp A, Simons A, Strauss M, Kemmling A, Oehler C, Cappai R, Pipkorn R, and Bayer TA. Possible mechanisms of APP-mediated oxidative stress in Alzheimer's disease. *Free Radic Biol Med* 33: 45–51, 2002.
38. Murphy MP, Echtay KS, Blaikie FH, Asin-Cayuela J, Cocheme HM, Green K, Buckingham JA, Taylor ER, Hurrell F, Hughes G, Miwa S, Cooper CE, Svistunenko DA, Smith RA, and Brand MD. Superoxide activates uncoupling proteins by generating carbon-centered radicals and initiating lipid peroxidation: studies using a mitochondria-targeted spin trap derived from alpha-phenyl-N-tert-butylnitrone. *J Biol Chem* 278: 48534–48545, 2003.
39. Nagai T, Sawano A, Park ES, and Miyawaki A. Circularly permuted green fluorescent proteins engineered to sense Ca^{2+}. *Proc Natl Acad Sci U S A* 98: 3197–3202, 2001.
40. Negre-Salvayre A, Hirtz C, Carrera G, Cazenave R, Troly M, Salvayre R, Penicaud L, and Casteilla L. A role for uncoupling protein-2 as a regulator of mitochondrial hydrogen peroxide generation. *FASEB J* 11: 809–815, 1997.
41. Nicholls DG and Ward MW. Mitochondrial membrane potential and neuronal glutamate excitotoxicity: mortality and millivolts. *Trends Neurosci* 23: 166–174, 2000.
42. Nicolakakis N, Aboulkassim T, Ongali B, Lecrux C, Fernandes P, Rosa-Neto P, Tong XK, and Hamel E. Complete rescue of cerebrovascular function in aged Alzheimer's disease transgenic mice by antioxidants and pioglitazone, a peroxisome proliferator-activated receptor gamma agonist. *J Neurosci* 28: 9287–9296, 2008.
43. Pecqueur C, Couplan E, Bouillaud F, and Ricquier D. Genetic and physiological analysis of the role of uncoupling proteins in human energy homeostasis. *J Mol Med (Berlin)* 79: 48–56, 2001.
44. Rousset S, Alves-Guerra MC, Mozo J, Miroux B, Cassard-Doulcier AM, Bouillaud F, and Ricquier D. The biology of mitochondrial uncoupling proteins. *Diabetes* 53(suppl 1): S130–S135, 2004.
45. Sastre M, Klockgether T, and Heneka MT. Contribution of inflammatory processes to Alzheimer's disease: molecular mechanisms. *Int J Dev Neurosci* 24: 167–176, 2006.
46. Sauer H, Wartenberg M, and Hescheler J. Reactive oxygen species as intracellular messengers during cell growth and differentiation. *Cell Physiol Biochem* 11: 173–186, 2001.
47. Simpson PB, Woollacott AJ, Moneer Z, Rand V, and Seabrook GR. Estrogen receptor ligands affect mitochondrial activity in SH-SY5Y human neuroblastoma cells. *Neuroreport* 13: 957–960, 2002.
48. Sompol P, Ittarat W, Tangpong J, Chen Y, Doubinskaia I, Batinic-Haberle I, Abdul HM, Butterfield DA, and St Clair DK. A neuronal model of Alzheimer's disease: an insight into the mechanisms of oxidative stress-mediated mitochondrial injury. *Neuroscience* 153: 120–130, 2008.
49. Stutzmann GE, Smith I, Caccamo A, Oddo S, Laferla FM, and Parker I. Enhanced ryanodine receptor recruitment contributes to Ca^{2+} disruptions in young, adult, and aged Alzheimer's disease mice. *J Neurosci* 26: 5180–5189, 2006.
50. Teshima Y, Akao M, Jones SP, and Marban E. Uncoupling protein-2 overexpression inhibits mitochondrial death pathway in cardiomyocytes. *Circ Res* 93: 192–200, 2003.
51. Tjalkens RB, Ewing MM, and Philbert MA. Differential cellular regulation of the mitochondrial permeability transition in an *in vitro* model of 1,3-dinitrobenzene-induced encephalopathy. *Brain Res* 874: 165–177, 2000.
52. Trenker M, Malli R, Fertschai I, Levak-Frank S, and Graier WF. Uncoupling proteins 2 and 3 are fundamental for mitochondrial Ca^{2+} uniport. *Nat Cell Biol* 9: 445–452, 2007.
53. Villarroya F, Iglesias R, and Giralt M. PPARs in the control of uncoupling proteins gene expression. *PPAR Res* 2007: 74364, 2007.
54. Vincent AM, Olzmann JA, Brownlee M, Sivitz WI, and Russell JW. Uncoupling proteins prevent glucose-induced neuronal oxidative stress and programmed cell death. *Diabetes* 53: 726–734, 2004.
55. Wang FS, Wang CJ, Chen YJ, Chang PR, Huang YT, Sun YC, Huang HC, Yang YJ, and Yang KD. Ras induction of

superoxide activates ERK-dependent angiogenic transcription factor HIF-1alpha and VEGF-A expression in shock wave-stimulated osteoblasts. *J Biol Chem* 279: 10331–10337, 2004.
56. Wang FS, Wang CJ, Sheen-Chen SM, Kuo YR, Chen RF, and Yang KD. Superoxide mediates shock wave induction of ERK-dependent osteogenic transcription factor (CBFA1) and mesenchymal cell differentiation toward osteoprogenitors. *J Biol Chem* 277: 10931–10937, 2002.
57. Wang W, Fang H, Groom L, Cheng A, Zhang W, Liu J, Wang X, Li K, Han P, Zheng M, Yin J, Wang W, Mattson MP, Kao JP, Lakatta EG, Sheu SS, Ouyang K, Chen J, Dirksen RT, and Cheng H. Superoxide flashes in single mitochondria. *Cell* 134: 279–290, 2008.
58. Zhang J, Liu Q, Chen Q, Liu NQ, Li FL, Lu ZB, Qin C, Zhu H, Huang YY, He W, and Zhao BL. Nicotine attenuates beta-amyloid-induced neurotoxicity by regulating metal homeostasis. *FASEB J* 20: 1212–1214, 2006.
59. Zhang K, Shang Y, Liao S, Zhang W, Nian H, Liu Y, Chen Q, and Han C. Uncoupling protein 2 protects testicular germ cells from hyperthermia-induced apoptosis. *Biochem Biophys Res Commun* 360: 327–332, 2007.
60. Zhang M, Wang B, Ni YH, Liu F, Fei L, Pan XQ, Guo M, Chen RH, and Guo XR. Overexpression of uncoupling protein 4 promotes proliferation and inhibits apoptosis and differentiation of preadipocytes. *Life Sci* 79: 1428–1435, 2006.

Address correspondence to:
Baolu Zhao
Institute of Biophysics
Chinese Academy of Sciences
15 Datun Road
Chaoyang District
Beijing 100101, the P.R. China

E-mail: zhaobl@sun5.ibp.ac.cn

Date of first submission to ARS Central, January 1, 2009; date of final revised submission, March 31, 2009; date of acceptance, April 10, 2009.